ISSN 1819-7140, Russian Journal of Pacific Geology, 2024, Vol. 18, No. 1, pp. 23–36. © Pleiades Publishing, Ltd., 2024.
Russian Text © The Author(s), 2024, published in Tikhookeanskaya Geologiya, 2024, Vol. 43, No. 1, pp. 27–41.

New Isotope-Geochemical Data on the Cenozoic Volcanism and the Geodynamics of the Underwater Vityaz Ridge (Pacific Slope of the Kuril Island Arc)

T. A. Emelyanova[a, *], Yu. A. Martynov[b, **†], N. S. Lee[a], and M. Yu. Davydova[b]

[a] *Il'ichev Pacific Oceanological Institute, Far Eastern Branch, Russian Academy of Sciences, Vladivostok, 6900041 Russia*
[b] *Far East Geological Institute, Far Eastern Branch, Russian Academy of Sciences, Vladivostok, 6900022 Russia*
**e-mail: emelyanova@poi.dvo.ru*
***e-mail: martynov@fegi.ru*

Received February 10, 2023; revised September 4, 2023; accepted September 26, 2023

Abstract—Original analytical data on trace elements and radiogenic Nd and Pb isotopes in the volcanic rocks of the Southern and southwestern part of the Northern plateaus of the underwater Vityaz Ridge are presented. Interpretation of these data and a comparison with published materials on the volcanic rocks from the southern and northern parts of the Kuril Island Arc (KIA), which formed on two basement blocks of different genetic nature, allow us to draw the following conclusions. The tholeiite varieties of volcanic rocks of the Southern Plateau and the southern part of the KIA have similar isotope-geochemical features, which point to the similar geodynamic conditions of the formation and the identical influence of low-temperature fluid on magma-generating processes. The geochemistry of the volcanic rocks of the Northern Plateau, which are mainly represented by subalkaline varieties, indicates a more pronounced contribution of the mantle component to the magmagenesis and a greater degree of influence of high-temperature melt compared to the rocks of the Southern Plateau, but a lesser degree compared to the rocks of the northern part of the arc. The volcanics of both plateaus are derivatives of a single mantle source, the MORB of the Indian Ocean (Indian MORB), and were formed together with the rocks of the southern part of the KIA within the lithospheric block transformed by tectonomagmatic processes that accompanied the opening of the Kuril Basin.

Keywords: radioisotope age, geochemistry, radiogenic isotopes, subduction, fluid, melt

DOI: 10.1134/S1819714024010020

INTRODUCTION

The underwater Vityaz Ridge is extended along the Pacific slope of the Kuril Island Arc (KIA) and separated from it by the inter-arc trough (Fig. 1). The ridge consists of the Southern (I) and Northern (II) plateaus, which are separated by a thick rifting zone, "a seismic gap of Central Kurils..." from a geophysical point of view [12, 22]. Previous geochronological (Table 1) and chemical studies of the volcanic rocks of the Vityaz Ridge established several volcanic stages that occurred in the Cenozoic, from Paleocene to mainly Pliocene–Pleistocene [5, 13, 15]. The Vityaz Ridge basement has a two-stage model age of 0.77 Ga [5], which is close to that of the Honshu Island in Japan (0.80 Ga), thus confirming the pre-existing point of view on the distribution of Precambrian basement beneath structures of the northwestern Pacific margin [20, 24].

The Pliocene–Pleistocene volcanic rocks of the Vityaz Ridge form underwater volcanoes, which coincide with positive magnetic anomalies [9]. The volcanoes are confined to transverse faults, which cut across the Vityaz Ridge, Kuril arc, and Kuril basin [23] and consist of tholeiitic, calc-alkaline, and subalkaline volcanic rocks ([5, 15], and others). Rocks of similar alkalinity were established at the Geophysicist Volcano, which is located in the eastern part of the Kuril basin [36]. In the earlier works, the cited authors suggested that tholeiitic and calc-alkaline varieties of Pliocene–Pleistocene volcanic rocks of the Vityaz Ridge in terms of alkalinity and some other geochemical characteristics are close to the analogous rocks of the Kuril arc, while subalkaline rocks, to those of the Kuril Basin [5]. Based on these data, it was concluded that the Vityaz Ridge is genetically related to the Kuril arc and eponymous basin. This fact provoked us to find new evidence to confirm or discard this relationship. The obtained new data on trace elements and radiogenic Nd and Pb isotopes in the volcanic rocks of the Vityaz Ridge may provide some insight into the nature of this structure, many genetic questions of which have remained open.

† Deceased.

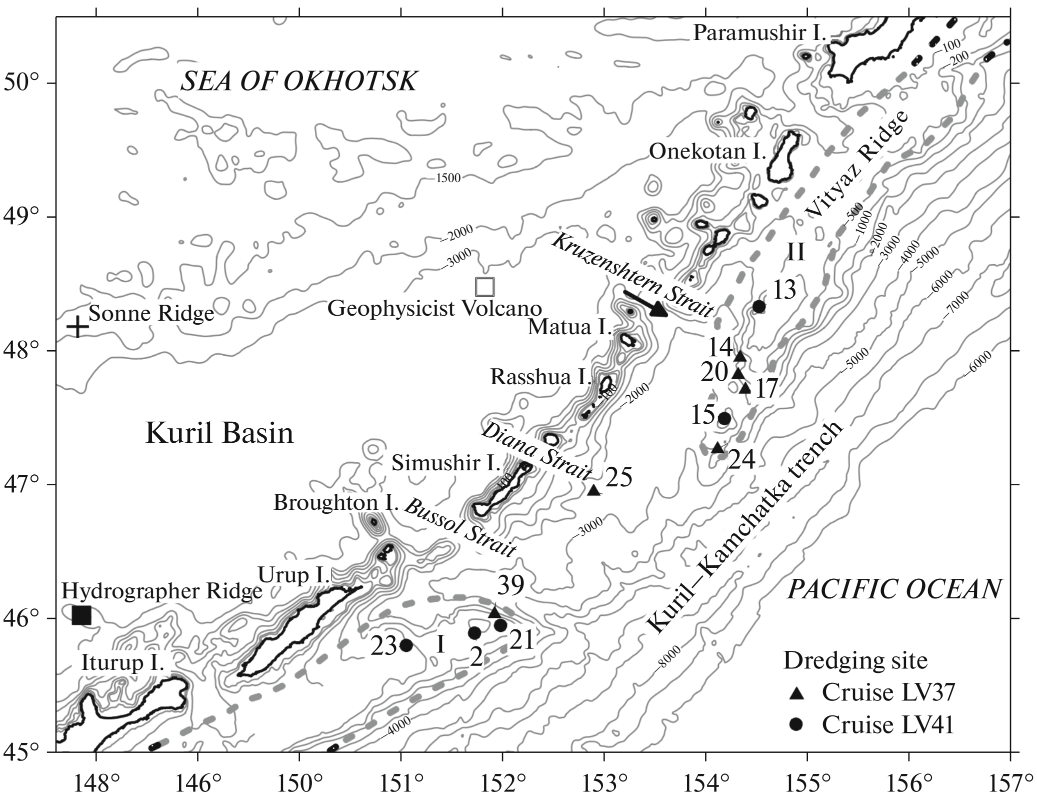

Fig. 1. A schematic map of the underwater Vityaz Ridge with dredging stations of the volcanic rocks (modified after [15]). Dashed lines and roman numerals show: (I) Southern Plateau and (II) Northern Plateau of the Vityaz Ridge. Arrow shows the boundary between the southern and northern parts of the Kuril island arc (modified after [19]).

METHODS

Samples of volcanic rocks were obtained by dredging of morphostructures of the underwater Vityaz Ridge during Cruises 37 and 41 of the R/V *Akademik M.A. Lavrentiev* in 2005 and 2006. The samples were dredged from steep slopes of seamounts and volcanoes located mainly in the central and peripheral parts of rifting zone (Fig. 1). The major and trace elements were determined in the volcanic rocks by "wet chemistry" and inductively coupled plasma mass spectrometry, respectively, on an ICP-MS Elan DRC II Perkin Elmer (United States) at the Kosygin Institute of Tectonics and Geodynamics of the Far Eastern Branch of the Russian Academy of Sciences (Khabarovsk); minerals were analyzed on an JXA-8100 at the Far East Geological Institute of the Far Eastern Branch of the Russian Academy of Sciences (Vladivostok). The geochronological age was determined by the K–Ar method on a MI-1201 IG mass spectrometer by isotope dilution using ^{38}Ar as spike at the Institute of Geology of Ore Deposits, Mineralogy, Petrography, and Geochemistry, Russian Academy of Sciences (Moscow). The Rb–Sr and Sm–Nd isotope studies were carried out at the Vernadsky Institute of Geochemistry and Analytical Chemistry, Russian Academy of Sciences, at the Laboratory of Isotope Geochemistry and Geochronology on a TRITON mass spectrometer (Moscow). The long-term reproducibility of isotope analysis was controlled using the SRM-987 international standard for Sr and La Jolla standard for Nd. The model age (T_{DM2}) was calculated relative to the mantle reservoir, with the present-day composition $\varepsilon_{Nd} = +9$ and Sm/Nd = 0.350 [11]. The description of previous analytical studies is reported in publication [5].

New trace-element (including rare-earth elements) and radiogenic Pb and Nd isotopes (Tables 2, 3, 4) were obtained in 2022. The major and trace element contents were determined at the Laboratory of the Analytical Chemistry of the Center for Collective Use of the Far East Geological Institute of the Far Eastern Branch of the Russian Academy of Sciences (Vladivostok). The contents of H_2O, L.O.I., and SiO_2 were measured by gravimetry; the FeO content was analyzed by titration (analysts L.I. Alekseeva and Zh.A. Shcheka). The elements were determined by inductively coupled plasma atomic emission spectrometry on an iCAP 7600Duo spectrometer (Thermo Scientific Corporation, United States), certificate no. 022219 on November 1, 2018. Analysts G.A. Gorbach, E.A. Tkallina, and N.V. Khurkalo. Trace elements were also analyzed using inductively coupled

Table 1. The results of geochronological dating of the volcanic rocks of the Vityaz Ridge

Ordinal No.	Sample No.	Latitude	Longitude	Dredging interval, m	K% ± σ, %	$^{40}Ar_{rad}$ ± σ, ng/g	Age ± 1.6 σ, Ma
1	Lv-41-13	48°19.86′	154°32.26′	380–240	1.73 ± 0.02	6.77 ± 0.05	55.5 ± 1.6
2	Lv-37-17-6	47°42.690′	154°23.208′	1770–1500	4.67 ± 0.05	16.55 ± 0.10	50.4 ± 1.2
3	Lv-37-14-4	47°57.019′	154°20.066′	1450–1200	1.92 ± 0.02	6.78 ± 0.09	50.2 ± 1.6
4	Lv-37-17-8	47°42.690′	154°23.208′	1770–1500	3.45 ± 0.04	11.45 ± 0.10	47.2 ± 1.4
5	Lv-37-24-2	47°16.015′	154°06.770′	1900–1700	2.23 ± 0.03	4.29 ± 0.11	27.5 ± 1.6
6	Lv-41-18-5	46°44.46′	152°39.06′	1880–1550	0.62 ± 0.015	0.625 ± 0.022	14.5 ± 1.2
7	Lv-37-37-6	45° 33.784′	151°33.306′	2200–1900	0.82 ± 0.015	0.607 ± 0.013	10.7 ± 0.6
8	Lv-41-23	45° 48.06′	151°03.00′	880–650	0.49 ± 0.015	0.147 ± 0.004	4.3 ± 0.3
9	Lv-41-24	45°46.01′	151°03.00′	660–610	1.39 ± 0.02	0.397 ± 0.004	4.1 ± 0.1
10	Lv-37-39-1	46°02.142′	151°55.161′	1600–1400	1.49 ± 0.02	0.341 ± 0.014	3.3 ± 0.3
11	Lv-37-25-1	46°56.958′	152°53.644′	1870–1600	0.30 ± 0.015	0.034 ± 0.003	1.6 ± 0.3
12	Lv-41-15-10	47°29.7′	154°10.86′	1125–790	1.31 ± 0.02	0.275 ± 0.003	3.0 ± 0.2

Volcanic rocks [15]. Paleocene–Miocene: (1) clinopyroxene–plagioclase basalts, (2) biotite–hornblende dacites, (3) basaltic andesite tuffs, (4) dacitic ignimbrites, (5–7) amphibole–two pyroxene–plagioclase andesites and dacitic andesites. (Pliocene–Pleistocene volcanic rocks): (8, 10) clinopyroxene–plagioclase basaltic andesites, (9) amphibole–two-pyroxene–plagioclase andesites, (11) olivine–clinopyroxene–plagioclase basalts, (12) amphibole–two pyroxene–plagioclase basaltic andesites.

plasma mass spectrometry on an Agilent 7700x spectrometer (Agilent Techn., United States), certificate no. 24631 on November 01, 2018. Results of element determination in rock samples are given in ppm. Samples for analysis were prepared by acid digestion ($HClO_4 + HNO_3 + HF$), analyst E.V. Volkova. Analysis was performed by M.G. Blokhin. Principal investigator N.V. Zarubina. The $^{143}Nd/^{144}Nd$, $^{206}Pb/^{204}Pb$, $^{207}Pb/^{204}Pb$, and $^{208}Pb/^{204}Pb$ isotope ratios were measured on a VG P54 multicollector spectrometer (MC-ICP-MS). JB-1b and JB-2 were used as standards for Nd and Pb, respectively. The Nd and Pb were separated using technique described in [28–30].

RESULTS AND DISCUSSION

Brief Geological–Geomorphological Overview

As mentioned, the Vityaz Ridge is split into the Southern and Northern plateaus by a thick destructive zone ([12, 22], and others), which is located between the Bussol and Diana straits (Fig. 1). This zone is extended through the entire central part of the Kuril island-arc system in the northwestern direction from the Kuril basin through the Kuril arc and Vityaz Ridge to the Kuril–Kamchatka trench, and can be termed as the Central Rift Zone (CRZ).

The Southern and Northern plateaus of the Vityaz Rudge are characterized by the stepped structure, and the surface of tectonic blocks is located at depths from 100 to 2000 m [13–15]. The ridge descends to the Kuril-Kamchatka trench in the southeast and toward the Middle Kuril trough in the northwest, which separates it from the Kuril Arc. Through the Bussol and Diana straits, the trough is connected with the Kuril Basin, with which it has almost equal maximum depth (3400–3500 m).

The Earth's crust in the Vityaz Ridge is subdivided into the continental (25–30 km), subcontinental (17–20 km), and oceanic (10–15 km) ones. The continental crust is typical of the Southern Plateau, the subcontinental, of the Northern Plateau, and oceanic, of the CRZ [7, 12, and others]. The thickness of the oceanic crust in the CRZ is reduced to 10–15 km, and the seismic wave velocity in the "basaltic" layer is 6.7–7.7 km/s [7]. It should be emphasized that the Earth's crust in the Kuril basin is also characterized by reduced thickness (up to 10–13 km), while the seismic wave velocity is 6.6–7.0 km/s, which is close to that of the CRZ [10, 12].

The geological basement of the Vityaz Ridge is made up of the pre-Upper Cretaceous and Upper Cretaceous–Lower Paleocene volcanogenic–siliceous–terrigenous rocks and Late Cretaceous granitoids [3, 14]. The pre-Cretaceous rocks are represented by metamorphosed sedimentary terrigenous and siliceous rocks: schists, hornfelses, and quartzites, as well as gabbroids (melanocratic gabbros, gabbrodolerites, dolerites, and diorites). The Late Cretaceous granitoid rocks (74.0 Ma) were found on the northwestern slope of the Northern Plateau and in the Bussol Strait and are represented by porphyritic biotite–hornblende granites and granodiorites [16, 17]. The Cenozoic sedimentary cover consists of Paleocene–Eocene coarse-clastic volcanogenic–terrigenous rocks, Oligocene–Upper Miocene tuffaceous diatomites, tuffaceous silty mudstones, tuffites, tuffs, and Pliocene–Pleistocene

Table 2. The contents of major (wt %) and trace (ppm) elements in the volcanic rocks of the Vityaz Ridge

Sample/ element	41-13	37-14-4	37-17-2	41-23	41-2	41-13-2	41-21	37-25-1	41-15-9	37-20-9
	1	2	3	4	5	6	7	8	9	10
SiO_2	52.32	55.33	52.64	51.77	49.10	54.39	54.90	53.84	50.00	54.47
TiO_2	0.88	0.77	0.80	0.56	0.90	0.98	0.82	0.72	0.69	1.17
Al_2O_3	15.86	15.54	16.90	19.57	17.20	15.86	18.01	18.00	20.04	15.94
Fe_2O_3	5.89	5.58	2.86	3.28	4.66	6.22	3.73	2.74	4.61	3.89
FeO	2.91	3.64	6.82	5.23	6.62	2.22	5.69	6.38	4.43	6.82
MnO	0.15	0.15	0.17	0.15	0.20	0.12	0.23	0.19	0.17	0.23
MgO	5.30	4.86	5.28	4.28	5.73	4.41	3.24	4.57	4.07	3.53
CaO	7.45	4.24	9.75	11.35	11.49	6.78	9.40	9.80	10.72	7.36
Na_2O	3.64	3.70	2.73	2.21	2.29	3.45	2.93	2.68	2.53	3.50
K_2O	1.87	2.23	0.39	0.42	0.35	1.76	0.40	0.36	0.34	0.74
P_2O_5	0.23	0.38	0.24	0.07	0.08	0.30	0.11	0.09	0.10	0.26
L.O.I.	1.73	2.86	1.21	0.8	1.04	1.83	0.50	0.48	1.38	1.51
Total	99.69	99.69	99.92	99.88	99.96	99.65	99.97	99.96	99.61	99.77
H_2O	1.46	0.42	0.12	0.18	0.31	1.33	–	0.11	0.54	0.34
Li	13.39	23.23	3.67	5.94	5.63	23.13	6.07	5.41	11.97	6.70
Be	0.74	0.98	0.28	0.21	0.26	0.98	0.38	0.23	0.28	0.61
Sc	32.61	21.55	36.94	33.16	44.54	24.19	36.83	38.49	28.57	34.03
V	302.5	237	298.7	250.5	404.1	241.6	279.4	315	283.3	198.9
Cr	80.54	34.76	20.88	20.17	7.63	61.11	7.35	28.91	15.61	3.44
Co	32.50	40.83	29.52	24.70	31.99	26.54	26.69	25.72	28.66	23.16
Ni	34.56	35.21	13.69	13.95	9.31	24.82	5.63	35.22	26.43	32.79
Cu	171.5	101.8	101.0	84.68	79.71	116.6	103.3	76.32	80.97	40.72
Zn	89.66	104.35	79.66	73.07	77.64	79.77	87.98	87.24	99.84	121.63
Ga	17.88	20.55	15.61	16.30	15.87	18.37	17.88	17.64	17.71	19.01
Ge	1.07	1.64	1.35	1.12	1.38	1.05	1.33	1.40	1.25	1.41
As	3.30	2.26	0.83	0.71	0.76	2.03	1.80	0.51	0.50	1.08
Rb	40.07	33.79	4.19	6.64	4.15	36.43	4.34	4.10	4.71	10.69
Sr	347.5	530.1	200.8	214.9	284.8	443.9	261.7	246.2	380.6	347.9
Y	15.88	21.12	25.55	14.94	18.27	17.86	21.74	16.99	16.29	30.53
Zr	69.04	62.82	47.43	38.86	33.15	114.3	47.89	36.24	29.30	78.36
Nb	2.06	1.99	0.56	0.44	0.57	3.20	0.75	0.51	0.56	1.45
Mo	0.44	0.37	0.49	0.74	0.63	0.63	1.47	0.84	0.49	0.82
Cd	2.68	0.21	0.16	3.10	0.09	0.26	0.10	0.09	3.62	0.32
Sn	2.34	0.95	1.00	1.76	0.55	1.23	0.75	1.63	0.72	1.03
Sb	0.26	0.28	0.19	0.17	0.14	0.36	0.23	0.16	0.14	0.25
Cs	0.99	0.48	0.32	0.39	0.24	1.39	0.12	0.19	0.15	0.44
Ba	529.58	1131	60.70	69.25	69.79	569.1	95.43	82.50	62.63	155.6
La	7.11	12.05	3.07	2.35	2.27	10.65	3.24	2.41	2.98	6.71
Ce	16.77	28.94	8.28	6.24	6.15	24.24	8.74	6.48	7.24	18.07
Pr	2.32	3.83	1.30	0.93	0.99	3.24	1.38	1.00	1.16	2.73
Nd	10.60	16.33	6.74	4.97	5.14	13.68	6.94	5.06	5.79	13.42
Sm	3.16	4.18	2.57	1.69	2.09	3.78	2.38	1.96	1.89	4.48
Eu	1.08	1.37	0.92	0.63	0.80	1.19	1.00	0.78	0.78	1.61

Table 2. (Contd.)

Sample/ element	41-13	37-14-4	37-17-2	41-23	41-2	41-13-2	41-21	37-25-1	41-15-9	37-20-9
	1	2	3	4	5	6	7	8	9	10
Gd	3.25	4.44	3.52	2.26	2.86	4.02	3.24	2.51	2.45	5.29
Tb	0.53	0.71	0.62	0.41	0.51	0.61	0.61	0.44	0.40	0.84
Dy	3.18	4.26	4.11	2.66	3.30	3.54	3.95	3.06	2.70	5.47
Ho	0.65	0.88	0.95	0.59	0.75	0.73	0.88	0.66	0.61	1.19
Er	1.94	2.56	2.91	1.80	2.25	2.11	2.55	1.97	1.84	3.50
Tm	0.27	0.35	0.41	0.25	0.32	0.30	0.38	0.30	0.26	0.49
Yb	1.62	2.39	2.77	1.75	2.12	1.92	2.55	2.00	1.71	3.33
Lu	0.25	0.37	0.44	0.27	0.31	0.28	0.40	0.32	0.27	0.52
Hf	1.90	1.89	1.44	1.15	1.07	2.68	1.45	1.16	0.90	2.26
Ta	0.13	0.13	0.05	0.03	0.05	0.22	0.06	0.04	0.04	0.09
W	0.43	0.34	0.31	0.28	0.13	0.35	0.22	0.17	0.16	0.11
Tl	0.02	0.72	<DL	<DL	<DL	0.01	<DL	<DL	<DL	0.02
Pb	6.42	7.15	3.54	2.99	3.70	8.72	3.66	3.42	2.55	4.41
Th	1.74	1.88	0.43	0.53	0.39	2.81	0.42	0.39	0.31	0.60
U	0.45	0.69	0.37	0.36	0.39	0.97	0.39	0.15	0.10	1.50

Determinations were made at the Laboratory of Analytical Chemistry of the Center for Collective Use of the Far East Geological Institute of the Far Eastern Branch of the Russian Academy of Sciences (Vladivostok) by inductively coupled plasma mass spectrometry on an Agilent 7700x spectrometer (Agilent Techn. United States). Sample preparation was made by acid digestion ($HClO_4 + HNO_3 + HF$). Analyst E.V. Volkova. Measurements were made by M. G. Blokhin. Principal investigator N.V. Zarubin. Volcanic rocks: (1, 3–5, 9) olivine–clinopyroxene–plagioclase basalts; (2, 6–8, 10) amphibole–two pyroxene–plagioclase basaltic andesites.

Table 3. The Nd isotope compositions of the volcanic rocks of the Vityaz Ridge

Sample no.	Volcanic rocks	$^{143}Nd/^{144}Nd$	Err	$\varepsilon_{Nd\,(0)}$
41-15-9	Olivine–clinopyroxene–plagioclase basalts	0.513040	3	7.8
41-2	"	0.512588	2	–1.0
41-23	"	0.513068	6	8.4
37-20-9	Amphibole–two pyroxene–plagioclase basaltic andesites	0.513069	2	8.4
41-21	"	0.513123	5	9.5
37-39-1	"	0.513000	4	7.1

Table 4. The Pb isotope compositions in the volcanic rocks of the Vityaz Ridge

Sample no.	$^{206}Pb/^{204}Pb$	±2s, %	$^{207}Pb/^{204}Pb$	±2s, %	$^{208}Pb/^{204}Pb$	±2s, %
41-15-9	18.257	0.06	15.504	0.09	38.090	0.12
41-2	18.408	0.06	15.516	0.09	38.241	0.12
41-23	18.404	0.06	15.524	0.09	38.277	0.12
37-20-9	18.317	0.06	15.488	0.09	37.993	0.12
41-21	18.396	0.06	15.524	0.09	38.237	0.12
37-39-1	18.380	0.06	15.499	0.09	38.141	0.12

diatom tuffites, tuffaceous diatomites, tuffaceous sandstones, and others [14, 25].

Cenozoic Volcanism

Tectonic processes within the Vityaz Ridge were accompanied by active volcanism [4, 5, 13-15]. During the period from 55.5 to 27.5 Ma (Table 1), which spans the Paleocene, Eocene, and Late Oligocene, volcanic stages frequently changed its nature depending on the shallow-water, deep-water, or subaerial environments at different parts of the ridge. However, subaerial volcanism was generally predominant, and its products were lavas and tuffs of clinopyroxene–plagioclase basalts and basaltic andesites, as well as felsic tuffs frequently welded up to ignimbrites, which are especially typical of Late Oligocene. According to the pre-existing point of view, the "green tuff" complex underlying the island-arc rocks of the Kuril arc was formed at that time [1, 21].

The Middle Miocene (14.5–10.7 Ma) within the ridge was responsible for outbursts of volcanism with formation of lavas and, more rarely, tuffs of amphibole–two pyroxene–plagioclase andesites ([4, 15], etc.). In general, the Middle Miocene volcanic rocks are ascribed to low-K calc-alkaline rocks, while their REE distribution pattern is almost unfractionated, which practically coincides with the REE patterns in the Middle Miocene volcanic rocks from the frontal zone of the KIA after [18]. However, the trace element patterns, although showing Ta–Nb and Ti negative anomalies, have very weakly expressed positive Sr and Zr positive anomalies, which are not typical of island-arc rocks. This can be explained by the peculiar conditions of formation of these rocks at the continent–ocean boundary and mixing of calc-alkaline magmas of continental margin with oceanic basaltic magmas.

Of most interest is the Pliocene–Pleistocene volcanism (4.3–1.6 Ma) widely developed on the Vityaz Ridge. The discovery of this young volcanic stage in 2006 discarded the previously existing point of view on the nonvolcanic nature of this structure [4, 5, 13–15]. The Pliocene–Pleistocene volcanic rocks form pillow-lavas and Fe–Mn crusts, which indicate their underwater formation and complete diving of the Vityaz Ridge beneath sea level in the Pliocene–Pleistocene. These rocks are represented by olivine–clinopyroxene–plagioclase and clinopyroxene–plagioclase basalts, amphibole–two pyroxene–plagioclase basaltic andesites, biotite–amphibole–two pyroxene–plagioclase andesites and dacitic andesites, with the predominance of basaltic andesites and andesites.

According to our previous [5, 13] and newly obtained data (Table 2), the SiO_2 contents in the described rocks vary from 49.10 to 61.90 wt %. The rocks are characterized by moderate and elevated Al_2O_3 contents and low contents of Fe-group elements (Ni, Cr, Co, and V). With increasing silica content, the rocks show accumulation of alkalis and decrease of contents of all other major elements. The level of alkalinity and K contents vary from low to elevated values lying within 3.07–5.75 and 0.40–2.18 wt %, respectively; Na_2O predominates over K_2O. Based on these facts, the Pliocene–Pleistocene volcanic rocks of the Vityaz Ridge are subdivided into tholeiitic, calc-alkaline, and subalkaline varieties, which in general are ascribed to the calc-alkaline series typical of geodynamic settings of island-arc (IAB) and active continental margins (ACMB). This is confirmed by the position of data points in the corresponding field in the discriminant diagram (Zr/Y)–(Nb/Y) ([5], etc.). This is additionally evidenced by low and moderate values of $(La/Sm)_N$, $(La/Yb)_N$, and Ti/V [5, 13]. The latter lies within 10–20, which corresponds to the island-arc rocks of the Kuril arc; some samples with high Ti/V ratios (up to 50) are similar to the volcanic rocks of the Kuril Basin.

In view of the isotope-geochemical comparison of Late Cenozoic volcanism of the Vityaz Ridge, Kuril Arc, and eponymous basin, it is necessary to mention that the arc by strike is subdivided into areas (or sectors). It has been accepted for many years that it consists of three sectors: the northern, central, and southern ones ([8], etc.).

This subdivision, with significant correction, could be supported by the presence of rifting zone found in the central part of the Kurils. However, based on isotope-geochemical data on the Quaternary volcanic rocks, the Kuril Arc can be subdivided into the southern and northern parts [19]. The evolution of the northern part is related to volcanism, which was contributed by the South Kamchatka heated and relatively depleted lithospheric block of the Pacific MORB-type. The magma generation within the southern part was caused by melting of "cold" isotopically enriched lithospheric mantle of the Indian MORB-type, which is depleted in trace elements due to Cenozoic tectonomagmatic processes of the Kuril basin opening. In Fig. 1, the arrow shows the boundary between these two parts (blocks).

A comparative analysis of new K_2O data on the volcanic rocks of the Southern Plateau showed its close concentrations with those in the rocks of the southern part of the KIA, while those of the Northern Plateau, with rocks of the northern segment of KIA (Fig. 2). In general, the majority of volcanic rocks of the ridge and arc are ascribed to the moderate-K rocks. However, one part of them demonstrates their similarity to the low-K field, while other, to the high-K fields. The comparison of the volcanic rocks of the ridge, arc, and Geophysicist Volcano located in the western part of the Kuril basin (Fig. 1) revealed the elevated K_2O contents in the subalkaline varieties. This similarity with basin rocks is best expressed in the rocks of the Northern Plateau and the northern part of the KIA. Much higher K contents are typical of the volcanic rocks of the Hydographer and Sonne ridges, which are represented by trachybasaltic andesites and trachyandesites [6, 38, etc.]. In terms of this parameter and some other isotope-geochemical features, they differ from other rocks of the basin, Vityaz Ridge, and Kuril arc.

Thus, the most similarity in terms of K_2O concentrations is observed between the subalkaline varieties of the Northern Plateau of the ridge, northern part of the arc, and Geophysicist volcano. Tholeiitic volcanic rocks of the Southern Plateau in terms of this parameter are close to the tholeiitic varieties from the southern segment of this part of the arc. The trachytic rocks of the Hydrographer and Sonne ridges in terms of the high total alkalinity and K content have no analogues within the Vityaz Ridge and KIA.

Before interpreting the trace element patterns (Fig. 3), it is important to emphasize the opposite Th and Hf behavior in revealing the nature of subduction components, which were involved in the reworking of melting mantle source and are represented by either low-temperature fluid or high-temperature melt. The former component is separated from sedimentary sequence of subducted oceanic plate during its dehydration, while the latter component, during its melting. Oceanic sediment is characterized by the large concentration of Th, which is immobile in aqueous fluid and easily passes into melt at sediment melting [33, 34]. Therefore, the minimum content of this element in the rocks indicates metasomatism by aqueous fluid while maximum content by melt; thereby, the Hf shows an opposite behavior.

In the multicomponent trace-element diagram, the volcanic rocks of the Southern and Northern plateaus of the Vityaz Ridge form negative Ta–Nb and Zr anomalies and positive Sr, Pb, and U anomalies, which is typical of the rocks of suprasubduction (including island-arc) settings (Fig 3a). However, tholeiitic volcanic rocks of the Southern Plateau show the better expressed Th minimum, which coincides with those of the analogous rocks of the frontal zone of the southern part of the arc (Fig. 3b). At the same time, the back-arc volcanic rocks practically have no Th anomaly, which indicates the higher concentrations of this trace element. The trace-element pattern of the volcanic rocks of the Northern Plateau shows both a well pronounced and a less pronounced Th minimum, as in the rocks of the northern part of the arc (Fig. 3c). This indicates that the high-temperature melt was involved in the formation of magmatic melts within the rear part of the arc, which was noted previously [18, 19, 32], while the low-temperature fluid operated in the frontal zone of the arc and the Southern Plateau of the Vityaz Ridge. Within the Northern Plateau and northern part of the arc, the magma genesis involved both fluid and melt.

The volcanic rocks of the Vityaz Ridge and Kuril basin show similar shapes of trace-element patterns for the subalkaline varieties of the ridge and Geophys-

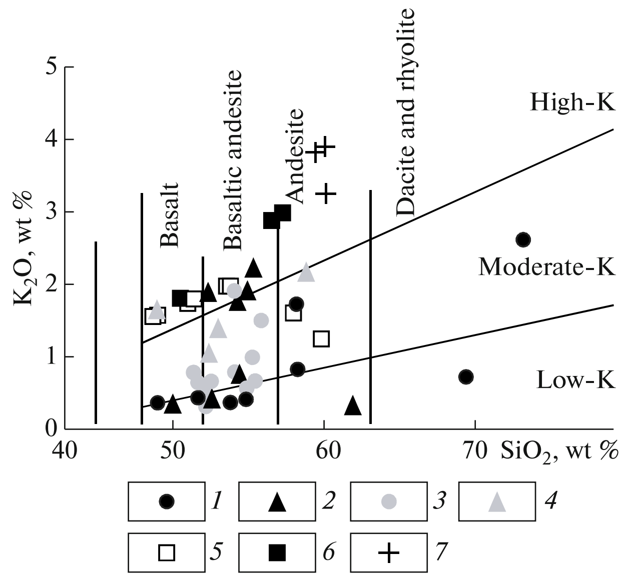

Fig. 2. The K_2O–SiO_2 classification diagram [31] for volcanic rocks: (*1*, *2*) Southern (*1*) and Northern (*2*) plateaus of the Vityaz Ridge (Table 2) and [5, 13]; (*3*, *4*) southern (*3*) and northern (*4*) parts of the Kuril arc [18]; (*5–7*) Kuril basin: (*5*) Geophysicist Volcano [26], (*6*) Hydrographer Ridge, and (*7*) Sonne Ridge [38].

icist Volcano (Fig. 3d), including also insignificant Th minimum, which indicates the contribution of high-temperature melt in the reworking of melting source. At the same time, the patterns of the volcanic rocks of the Hydrographer Ridge show the absence of Th anomaly and the less expressed Ta–Nb minimum. This is explained by the affiliation of the volcanic rocks of the latter to the trachytoid varieties, the geochemical and geodynamic specifics of which differ from those of other volcanic rocks of the described region.

The comparison of REE distribution patterns demonstrates that all volcanic rocks of the ridge are subdivided into the tholeiitic and calc-alkaline varieties with well and weakly pronounced negative Hf anomaly (Fig. 4a). The volcanic rocks of the Southern Plateau are comparable with tholeiitic rocks of the southern part of the arc (Fig. 4b). The rocks of the northern part of the KIA are ascribed to the more alkaline varieties and can be correlated only with some volcanic rocks of the Northern Plateau with similar alkalinity (Fig. 4c). A negative Hf anomaly is typical of volcanic rocks of the rear zone of this arc. This fact, in combination with the absence of Th minimum, is evidence for the contribution of a high-temperature subduction component (melt) to the genesis of back-arc lavas. The pattern of the frontal volcanic rocks of the arc shows no Hf anomaly. This means that the main role in the genesis of these magmas was played by the low-temperature fluid component. Within the Southern Plateau of the Vityaz Ridge and the southern part of the KIA, the Hf anomaly is absent (Fig, 4b), which

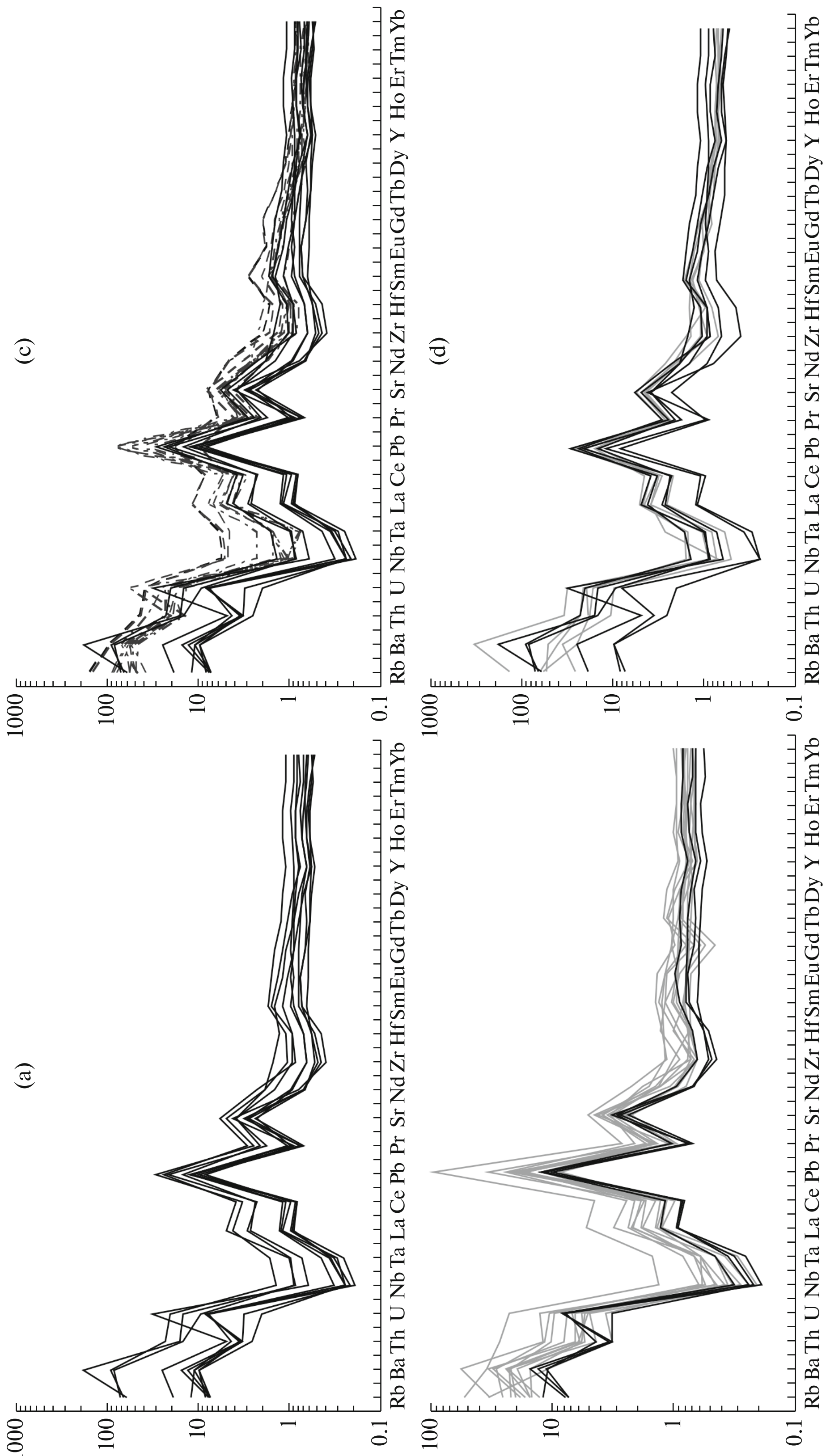

Fig. 3. The N-MORB-normalized [35] multicomponent trace-element patterns for the volcanic rocks of the Vityaz Ridge (a) compared to the volcanic rocks from the southern (b) and northern (c) parts of KIA [1] and Hydrographer (dashed line) and Geophysicist (dotted-dashed line) volcanoes of the Kuril basin (d) [26, 38]. Color of the patterns corresponds to that of data points in Fig. 2.

indicates the effect of low-temperature fluid on the magma generation. The volcanic rocks of the Northern plateau, in contrast, have a much better expressed negative Hf anomaly, which may indicate the contribution of high-temperature melt during magma generation within its limits (Fig. 4c).

Thus, the patterns of subalkaline varieties of the Northern Plateau are comparable with those of rocks of similar alkalinity of the Geophysicist Volcano of the Kuril Basin, but differ from sharply fractionated patterns of trachytoids of Hydrographer Ridge with well expressed LREE predominance over HREE (Fig. 4d). All subalkaline and alkaline volcanic rocks of the ridge and volcanoes of the Kuril basin show a negative Hf anomaly, which serves as an indicator of the influence of high-temperature melt on magma genesis. Thus, the pattern of most tholeiitic varieties of both plateaus of the ridge shows a flattening in the Hf region, and this fact argues in support of a low-temperature fluid.

Thus, the low Th and elevated Hf concentrations in the rocks of the Southern Plateau indicate the contribution of low-temperature fluid in the magma genesis, while the higher Th and low Hf concentrations in the rocks of the southern part of the KIA point to the contribution of high-temperature melt. The elevated Th and low Hf concentrations observed in some samples of the Northern Plateau indicate more intense activity of a high-temperature melt, which is not the case for the northern part of KIA, whose rocks are practically devoid of the negative Hf anomaly. The comparison of patterns of volcanic rocks of both plateaus of the Vityaz Ridge shows their similarity with rocks of the Geophysicist Volcano in the Kuril basin and clear difference from trachytoid rocks of the Hydrographer Ridge. However, the presence of a Hf minimum in all patterns of volcanic rocks of elevated alkalinity (including the Hydrographer Ridge) suggests the influence of high-temperature melt on magma genesis, which is not the case for tholeiitic varieties, whose magma genesis at the early stage was mainly controlled by low-temperature fluid.

The variations of the $^{143}Nd/^{144}Nd$ and Th/Nd ratios (Table 3, Fig. 5) once more emphasize the tholeiitic nature of the volcanic rock of the Southern Plateau, some basaltic samples of the Northern Plateau of the Vityaz Ridge, and rocks of the frontal zone of the KIA. The majority of the arc samples demonstrate similarity to rocks of the rear zone, which also includes the volcanic rocks of the basin: the Geophysicist Volcano and Hydrographer and Sonne ridges. In the first case, mantle metasomatism was mainly provided by the low-temperature fluid separated from altered oceanic crust. In the second case, the magma genesis was controlled not only by fluid but also by the high-temperature melts formed by melting of oceanic sediment at 650–800°C [19]. This is especially typical of the northern part of the arc, as well as the Hydrographer and Sonne ridges.

Mixing of the mantle and subduction components in magma-forming processes is illustrated by the ($^{206}Pb/^{204}Pb$)–($^{208}Pb/^{204}Pb$) diagram (Table 4, Fig. 6). The maximum contribution of enriched mantle (Indian MORB) was determined in the northwestern part of the Kuril Basin within the Sonne Ridge. All other volcanic rocks of the studied structures are derivatives of magmatic sources of mixed nature caused by the influence of fluid and melts of both oceanic sediment and altered oceanic crust. The rocks in the southern part of the arc and the Southern Plateau of the Vityaz Ridge were more affected by fluids and melts of oceanic sediment. The northern part of the arc and Northern Plateau strongly differ in this aspect: island-arc volcanic rocks are products of a source that was more reworked by fluids and melts compared to the volcanic rocks of the Vityaz Ridge, whose genesis was equally controlled by mantle and subduction components. This is also typical of the rocks of the Hydrographer Ridge and Geophysicist Volcano.

The interpretation of the Pb isotope data makes it possible to establish the nature of mantle sources beneath the Southern and Northern plateaus of the Vityaz Ridge. It is seen in the ($^{207}Pb/^{204}Pb$)–($^{206}Pb/^{204}Pb$) and ($^{206}Pb/^{204}Pb$)–($^{208}Pb/^{204}Pb$) diagrams (Figs. 7, 8) that data points of volcanic rocks of both plateaus fall in the field of the Indian MORB. Thus, the rocks of the Southern Plateau are localized near those of the southern part of the arc, together with which they are confined to the volcanic rocks of the Japan. The rocks of the Northern Plateau demonstrate different patterns, plotting in the field of Southern Kamchatka. The volcanic rocks of the Sonne Ridge fall in the Indian MORB, unlike the volcanic rocks of the Hydrographer Ridge and Geophysicist Volcano. In the first diagram (Fig. 7), they fall in the field of the Pacific MORB, which is consistent with the conclusions reported in [26, 27, 36, 38]. However, the $^{206}Pb/^{204}Pb$ and $^{208}Pb/^{204}Pb$ ratios (Fig. 8) show that the volcanic rocks of these structures are also ascribed to the Indian MORB derivatives.

These results indicate that the volcanic rocks of the Southern and Northern plateaus are ascribed to the island-arc rocks. The trace-element patterns show Ta–Nb and Zr minimums and Sr, Pb, and U maxima, which are characteristic feature of island-arc geodynamic setting. The REE pattern well illustrates the subdivision of rocks into tholeiitic and subalkaline varieties. The Southern Plateau is mainly characterized by tholeiitic volcanics, while the Northern Plateau comprises both varieties. From tholeiitic to subalkaline rocks, the Hf concentration decreases, while the Th concentration increases, which indicates the increasing role of high-temperature melt in the magma-generating processes, whereas low-temperature fluid played significant role at the initial stage.

Based on the Pb isotope relations, the mantle Indian MORB source was established beneath the

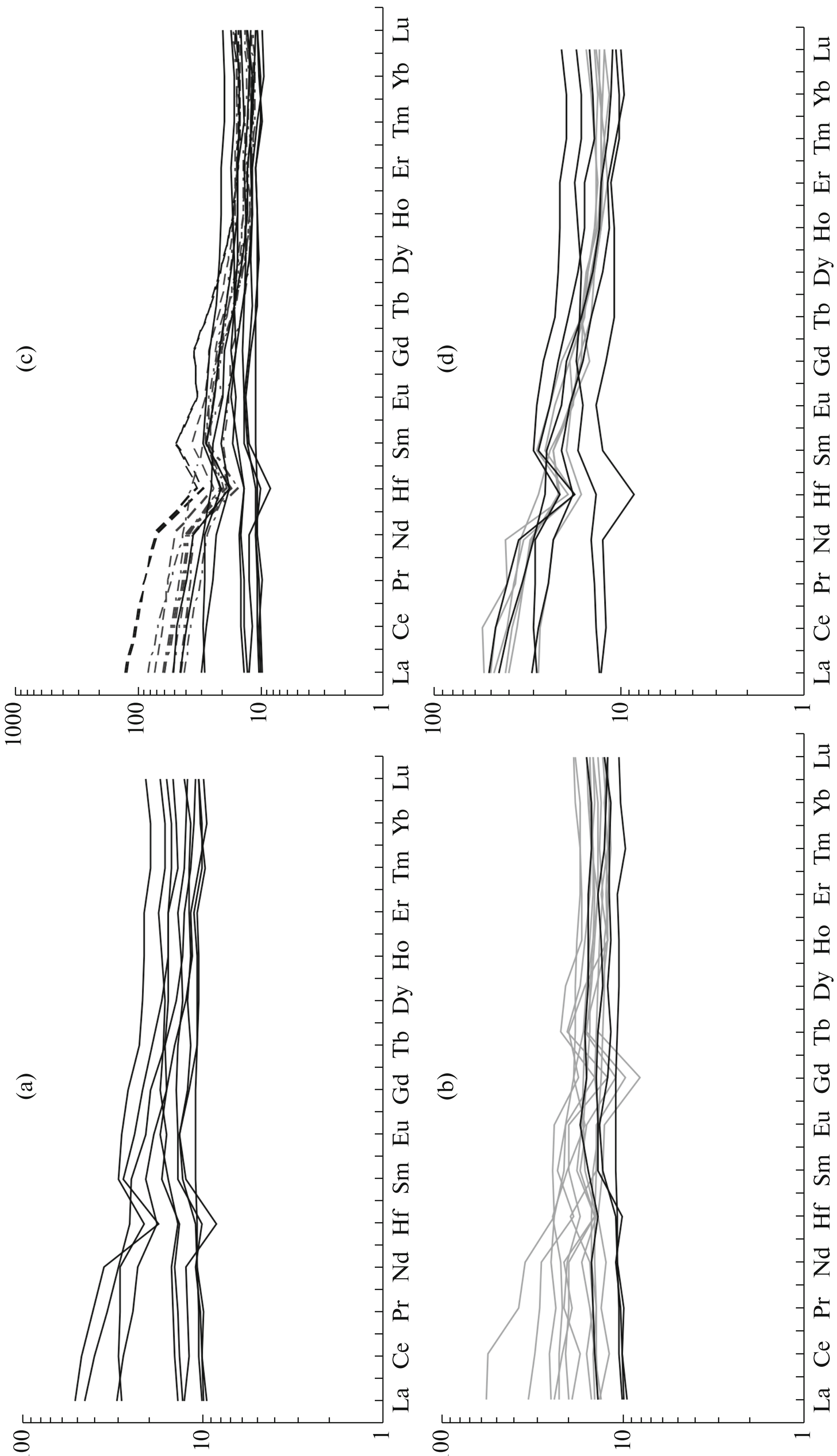

Fig. 4. The chondrite-normalized [35] REE and Hf distribution patterns. For symbols, see Figs. 2 and 3.

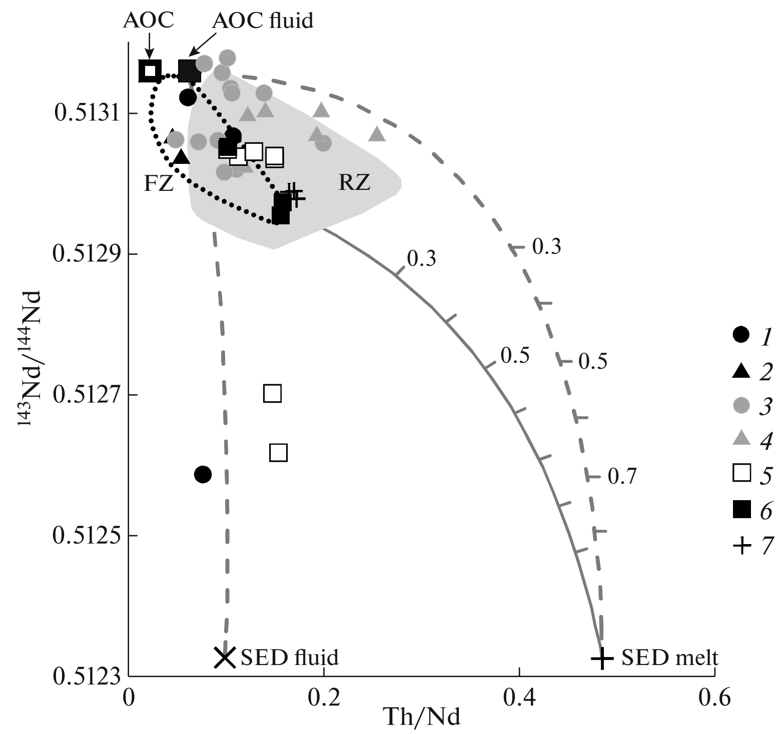

Fig. 5. Variations of the $^{143}Nd/^{144}Nd$ versus Th/Nd ratios [34] in the volcanic rocks of the Vityaz Ridge, Kuril Arc, and Kuril Basin. (AOC) altered oceanic crust; (AOC fluid) fluids formed through dehydration of altered oceanic crust; (SED fluid) dehydration of oceanic sediment; (SED melt) melt formed through melting of oceanic sediment. Outlines show: (FZ) frontal zone of KIA; (RZ) rear zone of KIA. Numerals in lines show proportions of mixing components (0.3-30% etc.). For symbols, see Fig. 2.

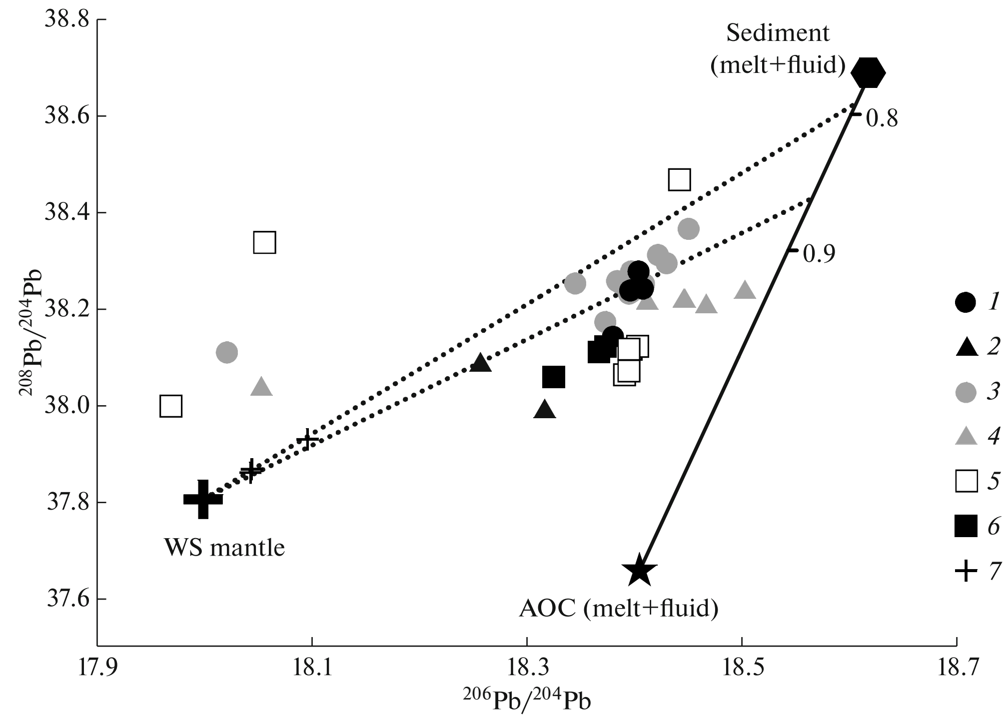

Fig. 6. The ($^{206}Pb/^{204}Pb$)–($^{208}Pb/^{204}Pb$) diagram for volcanic rocks from the Vityaz Ridge, Kuril Arc, and Kuril Basin, showing the calculated mixing curves of mantle and subduction components. (WS) Indian MORB mantle, AOC (melt+fluid) – altered oceanic crust (melt + fluid), Sediment (melt+fluid) – altered oceanic sediment (melt + fluid). Isotope compositions of mantle and subduction components are after [37]. Numerals show the proportions of mixing components. For symbols, see Fig. 2.

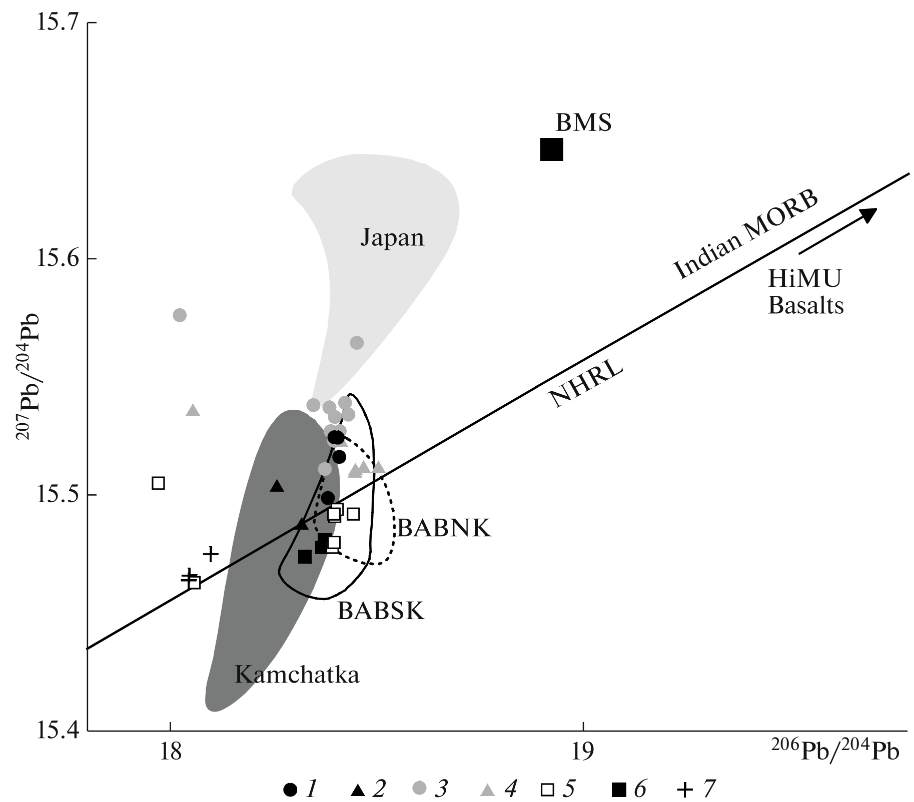

Fig. 7. The ($^{206}Pb/^{204}Pb$)–($^{207}Pb/^{204}Pb$) diagram for volcanic rocks of the Vityaz Ridge, Kuril Arc, and Kuril Basin. For symbols, see Fig. 2. Fields show back-arc lavas of the southern (solid line) and northern (dashed line) parts of KIA after [2]. BABSK and BABNK are basalts of the southern and northern areas of KIA, respectively. (BMS) bulk composition of oceanic sediment. NHRL (North Hemisphere Reference Line) is the curve of average compositions of basalts of the Northern Hemisphere.

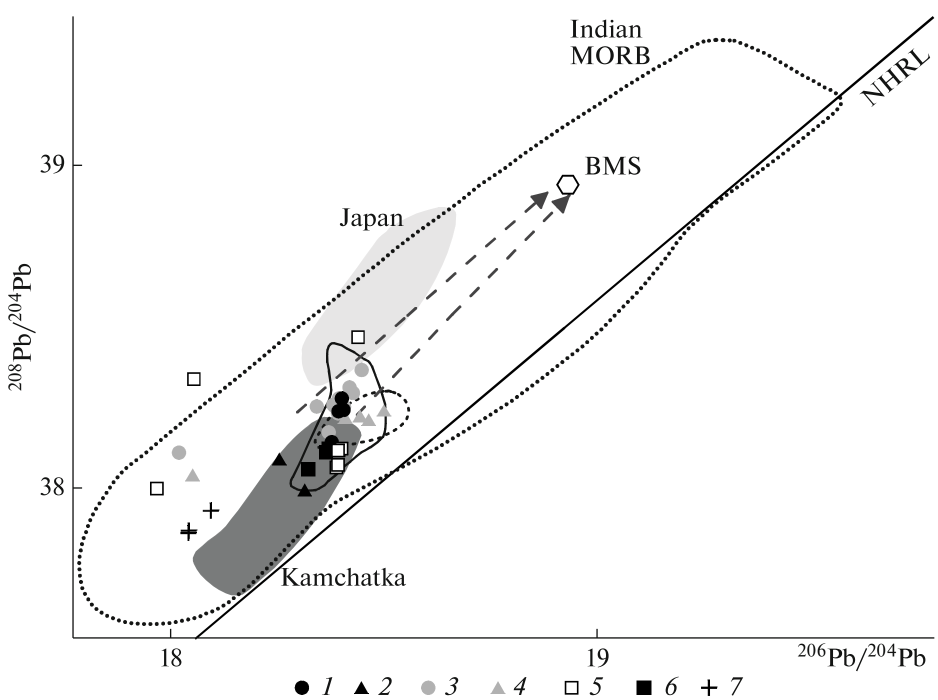

Fig. 8. The ($^{206}Pb/^{204}Pb$)–($^{208}Pb/^{204}Pb$) diagram for volcanic rocks of the Vityaz Ridge, Kuril Arc, and Kuril Basin. Dashed arrows are calculated mixing curves of mantle melts and sedimentary material. For symbols, see Figs. 2, 7.

Southern and Northern plateaus (Figs. 7, 8). This is inconsistent with conclusions that the northern part of the KIA is underlain by the Pacific MORB [19]. It was reasonable to suggest that the same source should be propagated also beneath the Northern Plateau of the Vityaz Ridge. However, this is not the case, which can be explained by the study of volcanic samples from the southwestern part of the Northern Pateau lying to the south of the boundary (Fig. 1, arrow) between two blocks of the KIA basement of different genetic nature [19].

Nevertheless, the isotope-geochemical features of volcanic rocks of the Southern and Northern plateaus of the Vityaz Ridge were compared with the rocks of corresponding areas of the arc. The highest geochemical similarity was established between tholeiitic rocks of the Southern Plateau and the southern part of the KIA. This is well seen in the multicomponent diagrams illustrating the trace-element composition (Figs. 3, 4). Figures 5, 6 demonstrate similar contributions of mantle and subduction components in the magma-generating processes, as well as the close degree of influence of the low-temperature fluid on these processes. At the same time, the role of high-temperature melt in the magma genesis of back-arc subalkaline volcanic rocks of the southern part of the arc increases.

The volcanic rocks of the Northern Plateau, in particular, its southwestern part, are represented by both tholeiitic and subalkaline varieties. Based on K_2O concentrations and the trace-element composition, the rocks of this plateau are close to the rocks of the northern part of KIA. This is also expressed in the Th and Hf behavior: an increase of Th and decrease of Hf contents from the tholeiitic to subalkaline volcanic rocks indicate an increasing role of high-temperature melt in the magma-forming processes (Figs. 3, 4). However, the Nd and Pb radiogenic isotopes were analyzed in tholeiitic varieties of basalts and basaltic andesites. Therefore, some difference is observed in the positions of data points of comparable structures in Figs. 5, 6, 7. The basalts of the Northern Plateau demonstrate a greater contribution of the mantle component and low-temperature fluid in the above-mentioned processes compared to the similar rocks from the northern part of the KIA.

CONCLUSIONS

New isotope-geochemical data on the volcanic rocks of the Southern Plateau and the southwestern part of the Northern Plateau of the Vityaz Ridge, as well as a comparative analysis suggest that all studied rocks are genetically related to the volcanic rocks of the southern part of the Kuril Island arc. The established Indian MORB mantle source was reworked by tectonomagmatic processes related to the opening of the Kuril Basin and subsequent subduction. The low-temperature fluid that separated during dehydration of subsiding slab played the predominant role at the early stages of the formation of tholeiitic lavas. The main role in the origination of the later alkaline volcanic rocks belonged to the high-temperature melt formed through melting of subduction sediment.

FUNDING

This work was financially supported by the Russian Science Foundation (project no. 23-27-00335) and was made in the framework of the government-financed project of the Il'ichev Pacific Oceanological Institute of the Far Eastern Branch of the Russian Academy of Sciences (no. 121021700342-9).

CONFLICT OF INTEREST

The authors of this work declare that they have no conflicts of interest.

REFERENCES

1. G. P. Avdeiko, O. N. Volynets, Yu. A. Antonov, V. I. Bondarenko, V. A. Rashidov, A. A. Tsvetkov, and N. G. Gladkov, "Catalogue of submarine volcanoes of the Kuril Island Arc," *Submarine Volcanism and Zoning of the Kuril Island Arc*, Ed. by Yu. M. Pushcharovsky (Nauka, Moscow, 1992), pp. 29–227 [in Russian].
2. G. P. Avdeiko, V. A. Rashidov, A. A. Poluvaeva, and I. M. Romanov, "Submarine volcanism of the Kurile Ridge: geodynamic conditions and formation of geochemical specifics," http://www.kscnet.ru/ivs/grant/grant_06/06-3-A-08-326/index.html (accessed January 02, 2009).
3. B. I. Vasil'ev, K. I. Sigova, and A. I. Obzhirov, *Geology and Petroleum Potential of the Marginal Seas of the Pacific Ocean* (Dal'nauka, Vladivostok, 2001) [in Russian].
4. T. A. Emelyanova and E. P. Lelikov, "Volcanism of the Okhotsk Sea and the Vityaz submarine ridge (Pacific slope of the Kurile arc)," *Far East Seas of Russia*, Ed. by V. A. Akulichev (Nauka, Moscow, 2007), **Vol. 3**, pp. 181–200 [in Russian].
5. T. A. Emelyanova, Yu. A. Kostitsyn, and E. P. Lelikov, "Geochemistry of the submarine Vityaz Ridge at the Pacific slope of the Kurile Island Arc," Geochem. Int. **50** (3), 289–303 (2012).
6. T. A. Emelyanova, A. M. Petrishchevsky, L. A. Izosov, N. S. Lee and A. A. Pugachev, "Late Mesozoic–Cenozoic stages of volcanism and geodynamics of the Sea of Japan and Sea of Okhotsk," Petrology **28** (5), 418–430 (2020).
7. S. M. Zverev and M. E. Polyanskii, "Structural variations along the Kuril–Kamchatka trench and a possible relation to seismicity," J. Volcanol. Seismol. **2** (1), 1–15 (2008).
8. T. K. Zlobin, V. N. Piskunov, and T. I. Frolova, "New data on the structure of the Earth's crust and central part of the Kuril Island Arc," Dokl. AN SSSR **293** (2), 185–187 (1987).
9. A. N. Ivanenko, A. M. Filin, A. G. Gorshkov, and N. A. Shishkina, "New data about the structure of the anomalous magnetic field in the central part of the Kuril–Kamchatka Island Arc," Oceanology **48** (4), 554–568 (2008).
10. I. P. Kosminskaya, S. M. Zverev, P. S. Veitsman, Yu. V. Tulikov, and R. M. Krakshina, "Main features of

the Earth's crust structure of the Kuril—Kamchatka zone of the Pacific ocean: evidence from deep-seismic sounding," Izv. AN SSSR, Ser. Geofiz., No. 1, 20–241 (1963).

11. Yu. A. Kostitsyn, "Terrestrial and chondritic Sm-Nd and Lu-Hf isotopic systems: are they identical?", Petrology **12** (5), 397–411 (2004).

12. R. G. Kulinich, B. Yu. Karp, B. V. Baranov, E. P. Lelikov, V. N. Karnaukh, M. G. Valitov, S. M. Nikolaev, T. N. Kolpashchnikova, and I. B. Tsoi, "Structural and geological characteristics of a "Seismic Gap" in the central part of the Kuril Island Arc," Russ. J. Pac. Geol. **26** (1), 3–14 (2007).

13. E. P. Lelikov, T. A. Emel'yanova, and B. V. Baranov, "Magmatism of the submarine Vityaz Ridge (Pacific slope of the Kuril Island Arc)," Oceanology **48** (2), 239–249 (2008).

14. E. P. Lelikov, I. B. Tsoy, T. A. Emel'yanova, E. P. Terekhov, N. G. Vashchenkova, N. K. Vagina, O. L. Smirnova, and V. D. Khudik, "Geological structure of the submarine Vityaz Ridge within the *seismic gap* area (Pacific slope of the Kurile Island Arc)," Russ. J. Pac. Geol. **27** (2), 99–109 (2008).

15. E. P. Lelikov and T. A. Emelyanova, "Geology and volcanism of the underwater Vityaz Ridge (Pacific slope of the Kuril Island Arc)," Oceanology **51** (2), 315–328 (2011).

16. E. P. Lelikov and T. A. Emelyanova, "Geochemistry of granitoids from the basement of the Kuril Island Arc System," Geochem. Int. **52** (8), 613–627 (2014).

17. E. P. Lelikov and T. A. Emel'yanova, "Granitoids in the basement of the Kurile island arc system," Dokl. Earth Sci. **454** (2), 123–127 (2014).

18. A. Yu. Martynov, Yu. A. Martynov, A. V. Rybin, and J. I. Kimura, "Rock of back-arc tectonics in the origin of subduction magmas: new Sr, Nd, and Pb isotope data from Middle Miocene lavas of Kunashir Island (Kurile Island Arc)," Russ. Geol. Geophys **56** (3), 363–378 (2015).

19. Yu. A. Martynov, A. I. Khanchuk, J.-I. Kimura, A. V. Rybin, and A. Yu. Martynov, "Geochemistry and petrogenesis of volcanic rocks in the Kuril Island Arc," Petrology **18** (5), 489–513 (2010).

20. M. A. Mishkin and G. M. Vovna, "Precambrian sialic crust of the Earth and its origin," Byull. Mosk. O-va Ispyt. Prir. **84** (5), 3–10 (2009).

21. B. N. Piskunov, *Geological—Petrological Specifics of the Island-Arc Volcanism*, Ed. by K. F. Sergeev (Nauka, Moscow, 1987) [in Russian].

22. Z. N. Proshkina, R. G. Kulinich and M. G. Valitov, "Structure, matter composition, and deep structure of the oceanic slope of the Central Kuril Islands: new evidence," Russ. J. Pac. Geol. **11** (6), 436–446 (2017).

23. K. F. Sergeev,*Tectonics of the Kurile Island Arc* (Nauka, Moscow, 1976) [in Russian].

24. A. I. Khanchuk, *Evolution of the Ancient Sialic Crust in the East Asian Island-Arc Systems* (DVNTs AN SSSR, Vladivostok, 1985) [in Russian]. 135 s.

25. I. B. Tsoy, "Oligocene—Early Miocene Silicoflagellates of the submarine Vityaz Ridge (island-arc slope of the Kurile—Kamchatka trench)," Al'gologiya, No. 1, pp. 111–125 (2011).

26. B. V. Baranov, R. Werner, K. A. Hoernle, I. B. Tsoy, P. Bogaard, and I. A. Tararin, "Evidence for compressionally induced high subsidence rates in the Kurile Basin (Okhotsk Sea)," Tectonophysics **350** (1), 63–97 (2002).

27. B. Baranov, H. K. Wong, K. Dozorova, B. Kimura, T. Ludmann, and V. Karnaukh, "Opening geometry of the Kurile Basin (Okhotsk Sea) as inferred from structural data," Island Arc **11** (3), 206–219 (2002).

28. S. Iizumi, K. Maehara, P. A. Morris, and Y. Sawada, "Sr isotope data of some GSJ rock reference samples," Mem. Faculty Sci. Shimane Univ. **28**, 83–86 (1994).

29. S. Iizumi, P. A. Morris, and Y. Sawada, "Nd isotope data for GSJ reference samples JB-1a, JB-3 and JG-1a and the La Jolla standard," Mem. Faculty Sci. Shimane Univ. **29**, 73–76 (1995).

30. J. -I. Kimura, M. Kawahara, and S. Iizumi, "Lead isotope analysis using TIMS following single column single bead Pb separation," Geosci. Rept. Shimane Univ. **22**, 49–53 (2003).

31. R. W. Le Maitre, S. L. Bateman, A. Dudek, et al., *A Classification of Igneous Rocks and Glossary of Terms* (Blackwell, Oxford, 1989).

32. Yu. A. Martynov, J. I. Kimura, A. I. Khanchuk, A. V. Rybin, A. A. Chashchin, and A. Yu. Martynov, "Magmatic sources of Quaternary lavas in the Kuril Island Arc: new data on Sr and Nd Isotopy," Dokl. Earth Sci. **417**, 1206–1211 (2007).

33. D. W. Peate and J. A. Pearce, "Causes of spatial compositional variations in Mariana Arc lavas: trace element evidence," Island Arc **7** (3), 479–495 (1998).

34. T. Plank and C. H. Langmuir, "Tracing trace elements from sediment input to volcanic output at subduction zones," Nature **362** (6422), 739–742 (1993).

35. S. S. Sun and W. F. McDonough, "Chemical and isotopic systematics of oceanic basalts: implications of mantle composition and processes," *Magmatism in the Ocean Basins*, Ed. by A. D. Saunders and M. J. Norry (Geol. Soc. Special Publ., London, 1989), pp. 313–345.

36. I. A. Tararin, E. P. Lelikov, and R. Werner, "Petrology and geochemistry of the volcanic rocks dredged from the geophysicist seamount in the Kuril Basin: evidence for the existence of thinned continental crust," Gondwana Res. **6** (4), 757–765 (2003).

37. D. Tollstrup, G. Gill, A. Kent, R. Williams, Y. Tamura, and O. Izhizuka, "Across-arc geochemical trends in the Izu-Bonin Arc: contribution from the subducted slab, revisited," Geochem. Geophys. Geosyst. **11** (1), paper Q01X10 (2010).

38. R. Werner, B. Baranov, K. Hoernle, et al., "Discovery of ancient volcanoes in the Okhotsk Sea (Russia): new constraints on the opening history of the Kurile back arc basin," Geosciences **10**, paper no. 442 (2020).

Recommended for publishing by A. A. Sorokin

Translated by M. M. Bogina